

PAPER • OPEN ACCESS

## Experimental and theoretical discussion on step-out characteristics of high temperature superconducting induction/synchronous motor

To cite this article: T Nakamura and D Sekiguchi 2019 *J. Phys.: Conf. Ser.* **1293** 012075

View the [article online](#) for updates and enhancements.

### You may also like

- [Investigation of crystallinity, mechanical properties, fracture toughness and cell proliferation in plasma sprayed graphene nano platelets reinforced hydroxyapatite coating](#)  
Swarnima Singh, Krishna Kant Pandey, O S Asiq Rahman et al.
- [SOFC Stack and System Development at Forschungszentrum Jülich](#)  
L. Blum, P. Batfalsky, Q. Fang et al.
- [PISCES-RF: a liquid-cooled high-power steady-state helicon plasma device](#)  
Saikat Chakraborty Thakur, Michael J Simmonds, Juan F Caneses et al.



**ECS**  
The  
Electrochemical  
Society  
Advancing solid state &  
electrochemical science & technology

**DISCOVER**  
how sustainability  
intersects with  
electrochemistry & solid  
state science research

# Experimental and theoretical discussion on step-out characteristics of high temperature superconducting induction/synchronous motor

T Nakamura and D Sekiguchi

Department of Electrical Engineering, Kyoto University, Kyoto 615-8510, Japan

nakamura.taketsune.2a@kyoto-u.ac.jp

**Abstract.** This paper presents experimental and theoretical results of step-out characteristics of a 20 kW class High Temperature Superconducting Induction/Synchronous Motor (HTS-ISM). A fabricated motor (3-phase, 8-pole, rotor windings: HTS, stator windings: Cu) is investigated, and its maximum quasi-synchronous output is 20 kW at line voltage of 400 V. The step out condition and its behaviour is investigated for different combinations of the input voltage and the drive frequency at 77 K (atmospheric liquid nitrogen). It is shown that tested results of torque versus primary current characteristics agree well with the theoretical expression by compensating with no-load currents. However, the corresponding step-out current differ each other when air-gap magnetic flux density, which is in proportion to (voltage/frequency), increases. Based on electromagnetic field analysis, it could be concluded the reason for the above discrepancy is the magnetic saturation of the iron core. Furthermore, step-out occurs at the phase angle of 45 degree regardless of which is whether or not the step-out current is affected by the above magnetic saturation. These results are really important for the consideration of stable rotation condition of the HTS-ISM.

## 1. Introduction

One of the advantages of superconducting rotating motor is its high power and/or high torque characteristics. For example, AMSC (USA) has succeeded in testing a 36.5 MW class ship propulsion motor [1]. The group of Kawasaki Heavy Industries et al. (Japan) has also succeeded in testing a 3 MW class motor [2].

The author's industry-university R&D cooperation group has been developing so-called High Temperature Superconducting Induction/Synchronous Motor (HTS-ISM) [3]. Although present mechanical output of our motor is smaller compared to the above reports, one of our main targets is realizing ultimately high power and/or torque density. In order to develop the higher power (torque) density motor, on the other hand, its step-out behavior should be investigated. When the load torque overcomes the generated torque of the motor, which doesn't possess any slip (asynchronous) torque, the motor suddenly stops, and then the motor transits to be a dangerous situation. Therefore, so-called overload tolerance for sudden experience of heavy load has to be clarified for the limit design of the motor. Such step-out characteristics are also crucial for the optimum control at the loaded condition.

In this paper, step-out phenomenon and condition are investigated for our fabricated 20 kW class HTS-ISM based on experiment and theoretical expression.





**Figure 1.** Photographs of a 20 kW class HTS-ISM [3].

**Table 1.** Specifications of a 20 kW class HTS-ISM [3].

Item	Stator	Rotor
Pole number	8	-
Number of slots	24	34
Inner diameter	160.0 mm	50.0 mm
Outer diameter	265.0 mm	159.4 mm
Length	200.0 mm	206.0 mm
Number of turns	30	-

## 2. Subject motor

A 20 kW class HTS-ISM is targeted in this study. Detailed explanation of the motor has already been reported in [3], and then basic structure and specifications of the motor is briefly shown in this section. Figure 1 and Table I, respectively, show a photograph and specifications of the developed 20 kW class HTS-ISM. A 3-phase and 8-pole stator structure is adopted and the rated voltage is 400 V. A Bi-2223 squirrel-cage rotor is coupled with conventional (copper) stator, and then the tests are carried out in atmospheric liquid nitrogen (77 K). It should be noted that the motor doesn't possess any slip (asynchronous) torque [3].

## 3. Theoretical expression of maximum output and step-out condition

### 3.1. Expression of torque of HTS-ISM

Rotating principle of the HTS-ISM is similar to that of squirrel-cage induction motor [4]. Therefore, characteristics of the motor can be discussed based on an electrical equivalent circuit that is commonly adopted for describing performance of conventional motor.

Figure 2(a) shows an electrical equivalent circuit of the HTS-ISM, of which  $r_1$  is primary winding's resistance and  $x$  is leakage reactance.  $V_2'$  is the HTS rotor winding's voltage drop that is converted to the primary side, and it shows nonlinearity depending upon current ( $I_1 = I_2'$ ). In order to derive intuitively clear expression of the motor's maximum output, exciting circuit is neglected in this study. From this circuit, the torque of the HTS-ISM ( $\tau$ ) is expressed as follows [4].

$$\tau = 3 \frac{P}{\omega} \Phi_2' I_2' \quad (1)$$

$$\Phi_2' = \frac{\sqrt{V_1^2 - x^2 I_2'^2 - r_1^2 I_2'^2}}{\omega} \quad (2)$$

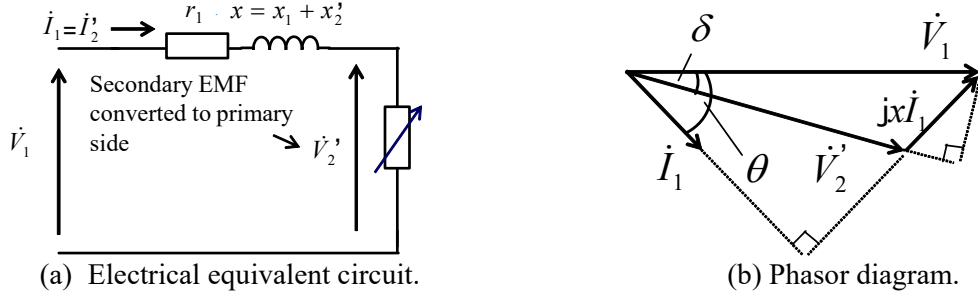


**Figure 2.** One phase phasor expression of an HTS-ISM.

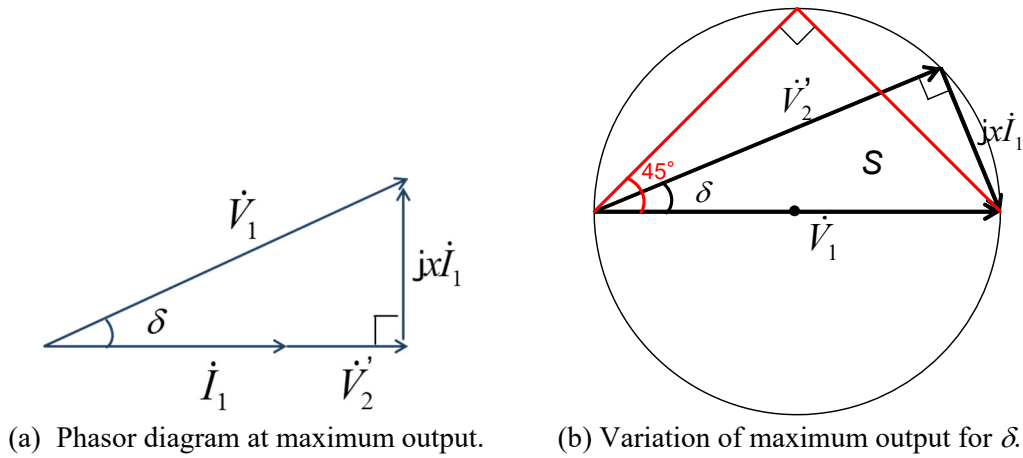


**Figure 3.** Explanation of step-put based on phasor diagram.

where,  $\Phi_2'$  is secondary magnetic flux that is converted to primary side. As can be seen in equations (1) and (2),  $t$  shows its maximum value for the  $I_2'$ .

### 3.2. Maximum output and Step-out condition

Figure 2(b) illustrates the phasor diagram obtained from figure 2(a). Where,  $\theta$  denotes angle between  $V_1$  and  $I_1$ , and  $\delta$  between  $V_1$  and  $V_2'$ . It should be noted that  $r_1$  is neglected for this diagram in order to realize clear discussion. From the diagram, we can express the output ( $P$ ) as follows.

$$P = 3V_2' I_1 \cos(\theta - \delta) \quad (3)$$

From equation (3), the following relation must be satisfied for the maximum output ( $P_M$ ).

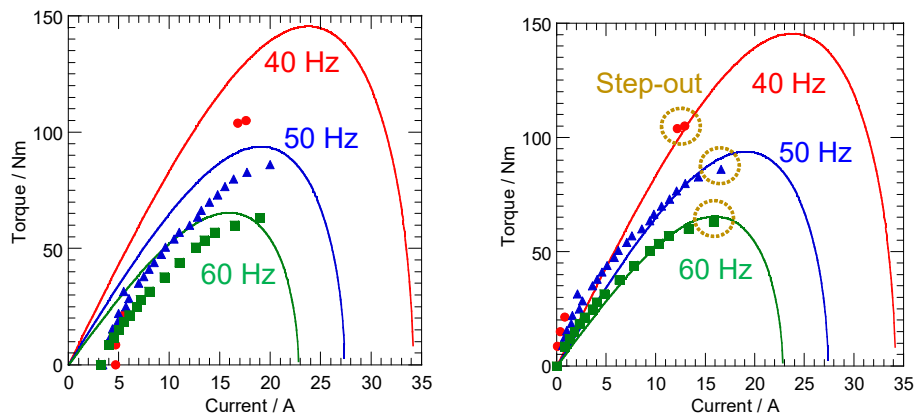
$$\theta = \delta \quad (4)$$

Figure 3(a) illustrates the phasor diagram for  $P_M$ , and it is expressed as follows.

$$P_M = 3V_2' I_1 = 3 \frac{V_2' V_1}{x} \sin \delta \quad (5)$$

$$\sin \delta = \frac{x I_1}{V_1} \quad (6)$$

Furthermore, the above  $P_M$  will be changed by the mechanical load as shown in figure 3(b), and then the threshold for the stable rotation is determined at  $\delta=45^\circ$  degree, of which  $P_M$  becomes  $3V_1^2/2x$  ( $I_1 = V_1/\sqrt{2}x$ ). In other word, this angle gives the step-out condition of the motor. In this paper, validity of the aforementioned condition for the 20 kW class HTS-ISM is investigated.



(a) Without no-load current compensation. (b) With no-load current compensation.

**Figure 4.** Torque versus current curves (77 K).

## 4. Results and discussion

### 4.1. Load characteristics

Figure 4 shows torque ( $\tau$ ) versus current ( $I_1$ ) curves for different frequencies (solid curves: theoretical expression, symbols: tested results). As can be seen in the figure 4(a), although the obtained torque increases with the current before the motor steps out, such values differ from the theoretical expressions. Main reason for this discrepancy would be come from the no-load current. That is, no-load current is included in the current even such current doesn't contribute to the torque. Therefore, the no-load current is simply subtracted from the tested results, and then the results are shown in figure 4(b). As shown in the figure, the tested results agree well with the theory.

### 4.2. Step-out phenomenon

Step-out currents are marked with open circles in figure 4(b). We can see that the tested step-out current (marked by open circles) agree with the theoretically obtained maximum torque when the frequency is higher. However, discrepancy between the test and the theory becomes distinct by decreasing the frequency. It is known that the air-gap magnetic flux density is in proportion to voltage ( $V_1$ )/frequency ( $f$ ), and then such flux will increases by decreasing the frequency at the fixed value of the voltage. In other words, the magnetic saturation would occur in the iron core when  $V_1/f$  increases. Figure 5 shows temporal traces of primary current ( $I_1$ ) and phase angle ( $\theta$ ) for different voltages at 50 Hz. It should be noted that the initial value of phase angle is about 45 degree for both conditions and the motor is in a step-out mode. Then, the step-out occurs at 176.6 s for  $V_1 = 320$  V and 217.2 s for  $V_1 = 400$  V. Although both of  $I_1$  and  $\theta$  shows smooth trace for the case of lower voltage (320 V), such traces vibrate for the higher voltage (400 V). Possible reason for the vibration would also be the magnetic saturation.

In order to validate above assumption, magnetic field analysis (2D finite element method) is carried out for the condition of 400 V/50 Hz as shown in figure 6. Figure 6(a) shows magnetic flux density contour of the core, and its highest value reaches more than 1.5 T. Therefore, the iron core will be in saturation state for this condition. The corresponding current waveforms are also shown in Fig. 6(b), and they are largely distorted due to the above magnetic saturation. That is to say, inclusion of harmonic component due to the magnetic saturation would be the reason for the vibration of current waveform, and also that for the discrepancy of step-out current between the test and the theory.

Furthermore, figure 7 shows step-out angle for various conditions of  $V_1/f$  and torque. As can be seen in the figure, the step-out angle always less than 45 degree, as is expected by the conventional theory (figure 3(b)). Namely, the theoretical condition for the step-out angle, fortunately, is always valid to be 45 degree without dependence of the aforementioned magnetic state of the iron core. Based

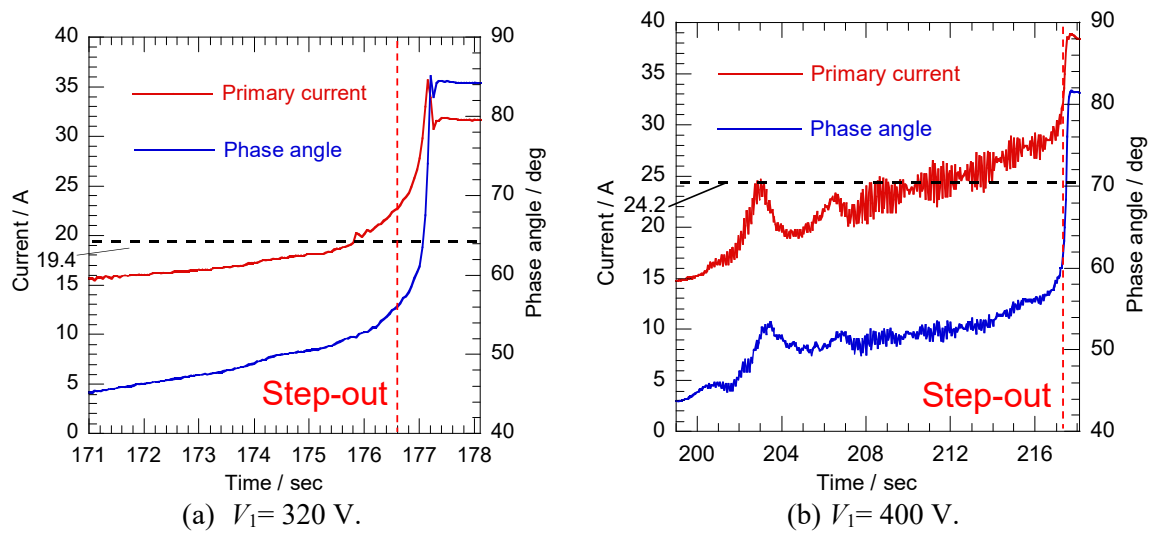


**Figure 5.** Temporal traces of primary current and phase angle for different voltages at 50 Hz.

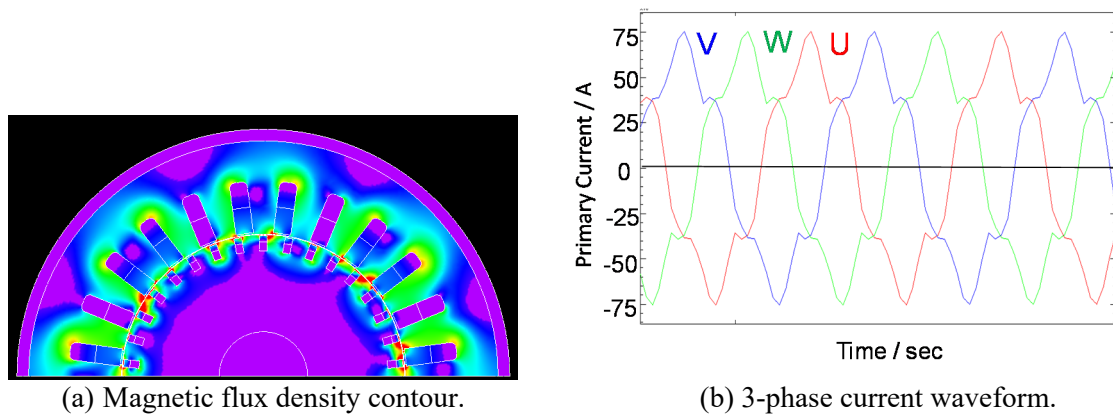


**Figure 6.** 2D electromagnetic field analysis for condition of 400 V/50 Hz.

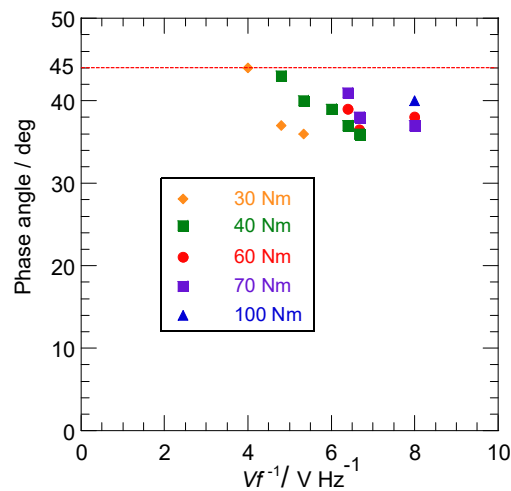


**Figure 7.** Step-out angle for various conditions of  $V_1/f$  and load torque.

on this condition, we have to design or set the operational condition with a safety margin, which depends on applications. This will be one of our future works. It should be noted that the basic mechanism of step-out phenomenon of the HTS-ISM discussed in this paper is same as that of conventional motors.

## 5. Conclusion

In this paper, step-out characteristics are tested and then discussed based on nonlinear equivalent circuit. It was shown that the tested results of torque versus current curves agree with the theoretical expressions by compensating with the no-load current. Step-out current differs from the theory and the reason for this would be magnetic saturation of the iron core. Even in the above problems, the step-out phenomenon always occurs when the phase angle becomes more than 45 degree as expected by the conventional theory. This results would be effective for the reliable and safe operation of the HTS-ISM.

## Acknowledgments

This work was supported by Japan Science and Technology Agency under the program of Advanced Low Carbon Technology Research and Development Program (JST-ALCA) in Japan.

## References

- [1] Gamble B, Snitchler G and MacDonald T 2011 Full Power Test of a 36.5 MW HTS Propulsion Motor *IEEE Trans. Appl. Supercond.* **21**(3) 1083-1088
- [2] Yanamoto T, Izumi M, Umemoto K, Oryu T, Murase Y and Kawamura M 2017 Load test of 3-MW HTS motor for ship propulsion *IEEE Trans. Appl. Supercond.* **27**(8) 5204305
- [3] Nakamura T, Itoh Y, Yoshikawa M, Nishimura T, Ogasa T, Amemiya N, Ohashi Y, Fukui S and Furuse M 2015 Tremendous enhancement of torque density in HTS induction/synchronous machine for transportation equipments *IEEE Trans. Appl. Supercond.* **25**(3) 5202304
- [4] Morita G, Nakamura T and Muta I 2006 Theoretical analysis of a YBCO squirrel-cage type induction motor based on an equivalent circuit *Supercond. Sci. Technol.* **19**(6) 473-478